# Bridging between load-flow and Kuramoto-like power grid models: A flexible approach to integrating electrical storage units

Cite as: Chaos **29**, 103151 (2019); https://doi.org/10.1063/1.5099241
Submitted: 08 April 2019 . Accepted: 16 August 2019 . Published Online: 31 October 2019

Katrin Schmietendorf, O. Kamps, M. Wolff, P. G. Lind, P. Maass, and J. Peinke

# Bridging between load-flow and Kuramoto-like power grid models: A flexible approach to integrating electrical storage units

Cite as: Chaos **29**, 103151 (2019); doi: 10.1063/1.5099241
Submitted: 8 April 2019 · Accepted: 16 August 2019 ·
Published Online: 31 October 2019



Katrin Schmietendorf,[1,a)] O. Kamps,[2] M. Wolff,[3] P. G. Lind,[4] P. Maass,[3] and J. Peinke[1]

## AFFILIATIONS

[1]ForWind and Institut für Physik, Universität Oldenburg, Küpkersweg 70, 26129 Oldenburg, Germany
[2]Center for Nonlinear Science, Universität Münster, Correnstraße 2, 48149 Münster, Germany
[3]Fachbereich Physik, Universität Osnabrück, Barbarastraße 7, 49076 Osnabrück, Germany
[4]Department of Computer Science, Oslo Metropolitan University, P.O. Box 4 St. Olavs plass, N-0130 Oslo, Norway

**Note:** This paper is part of the Focus Issue on the Dynamics of Modern Power Grids.
[a)]**Electronic mail:** katrin.schmietendorf@uni-oldenburg.de

## ABSTRACT

In future power systems, electrical storage will be the key technology for balancing feed-in fluctuations. With increasing share of renewables and reduction of system inertia, the focus of research expands toward short-term grid dynamics and collective phenomena. Against this backdrop, Kuramoto-like power grids have been established as a sound mathematical modeling framework bridging between the simplified models from nonlinear dynamics and the more detailed models used in electrical engineering. However, they have a blind spot concerning grid components, which cannot be modeled by oscillator equations, and hence do not allow one to investigate storage-related issues from scratch. Our aim here is twofold: First, we remove this shortcoming by adopting a standard practice in electrical engineering and bring together Kuramoto-like and algebraic load-flow equations. This is a substantial extension of the current Kuramoto-like framework with arbitrary grid components. Second, we use this concept and demonstrate the implementation of a storage unit in a wind power application with realistic feed-in conditions. We show how to implement basic control strategies from electrical engineering, give insights into their potential with respect to frequency quality improvement, and point out their limitations by maximum capacity and finite-time response. With that, we provide a solid starting point for the integration of flexible storage units into Kuramoto-like grid models enabling to address current problems like smart storage control, optimal siting, and rough cost estimations.



**The Kuramoto model describes the phase dynamics of coupled oscillators and is a paradigm for self-organized synchronization. Synchronization also plays a crucial role in power system operation. Against this backdrop, Kuramoto-like power grid models are used to investigate grid stability and dynamics. Short-term feed-in fluctuations by wind and solar plants are known to induce frequency fluctuations and, therefore, pose a major challenge to frequency quality. Electrical storage is the key technology for balancing these fluctuations and ensure power quality. In order to address this issue with Kuramoto-like grids, we extend the modeling framework by storage units with arbitrary control schemes. With this, Kuramoto-like grids can be used to investigate different aspects of storage integration like optimal embedding and smart novel control schemes, which are able to cope with the turbulentlike nature of wind and solar.**

## I. INTRODUCTION

The transition of the electrical energy system toward sustainability is paralleled by grid decentralization and increasing percentage of renewables. This development requires novel grid operation and design concepts. Electrical storage will be a key component of future energy systems to balance feed-in variations and mitigate

power quality problems induced by stochastic renewables.[1–3] Therefore, new research issues emerge concerning optimal grid embedding and sizing of storage facilities as well as smart storage-control strategies, which are customized to the specific application purpose and feed-in properties.

Wind and solar have characteristic non-Gaussian statistics over a broad range of time scales from seasonal and diurnal imbalances down to subsecond fluctuations.[3,4] Short-term fluctuations on the second and subsecond scale are a particular challenge for power system operation, since standard load balancing such as primary control[5] does not operate yet on these time scales. As a consequence, frequency quality is significantly reduced.[1,2,6] This problem is exacerbated by a side effect: renewables are typically connected to the grid via inverters. On the one hand, the replacement of conventional generators leads to a decrease of system inertia, and, therefore, the grid becomes more sensitive to sudden perturbations in terms of feed-in fluctuations. On the other hand, inverters have different dynamical features than synchronous machines, as they are not governed by an inherent physical relationship to the frequency.[7–9]

Against this backdrop, there is a growing interest in short-term dynamics and multidisciplinary approaches including self-organization and collective phenomena. This requires a profound mathematical modeling framework mediating between the simple conceptual models from nonlinear dynamics and the detailed models used for case studies in electrical engineering. Over the past decade, the Kuramoto-like modeling framework has been established as a suitable instrument for this purpose. It is derived from the original Kuramoto model, which describes the phase dynamics of coupled oscillators, in particular, the phase transition from incoherence to self-organized synchronization.[10,11] Kuramoto-like models have been used to address various issues of power system dynamics and topology-stability interplay.[12–19] In a previous work,[6] it was shown how the turbulentlike character of wind feed-in, in particular, its intermittency, is directly transferred into frequency and voltage fluctuations. This was confirmed by real-world frequency measurements.[20,54] Other recent studies on Kuramoto-like grids with stochastic feed-in investigated the propagation of frequency quality deterioration[21,22] and potential routes to system instability.[23] However, the current Kuramoto-like framework does not allow implementing grid components, which are not modeled by oscillator equations. This shortcoming affects the integration of storage units with arbitrary control strategies from scratch and hence prevents from fundamental investigations of storage-related issues.

With our study, we fill this gap. The primary target was to integrate a flexible storage model, which does not imply any restrictive assumptions on storage features or control strategies beforehand. For this purpose, we introduce a novel approach by bringing together Kuramoto-like differential and algebraic load-flow equations, which are a standard tool in power-flow analysis. The general idea of embedding grid components by means of load-flow equations has a broader range of application: it can serve as a starting point to implement arbitrary grid components into Kuramoto-like power grids, e.g., power inverters with various types of control or nodes connecting different grid levels. This broadens the scope of Kuramoto-like models significantly. At the same time, the modeling framework is still a reduced approach compared to the detailed models used in electrical engineering and yet simple enough to address power grid dynamics from the viewpoint of self-organization and collective dynamics, i.e., methods beyond the standard engineering practice.

For demonstration purposes, we consider frequency quality improvement by means of a storage facility with limited capacity in a simplified power system subjected to realistic wind feed-in. This application example has been identified as one of the key issues on the road to power systems with high percentage of wind and solar by electrical engineering communities.[1,2,24–26] Against this context, our problem setting refers to a current standard control problem in electrical engineering and control theory. Jabir *et al.*[25] and Zhao *et al.*[26] provide an overview on different smoothing approaches for wind power applications. Jabir *et al.* identify battery storage as the most promising candidate for effective power quality management, which, however, still can be improved by new control strategies. Li *et al.*[27] considered a hybrid battery storage system with a novel state-of-charge based control strategy for smoothing power output fluctuations. Lee *et al.*[28] investigated the limitation of ramp rates of wind power by means of a storage system with stochastic optimal control. Hamsic *et al.*[29] studied the introduction of a flywheel storage system into an isolated power system including wind turbines. A novel control concept for the integration of renewables was proposed by Hesse *et al.*[30] in the form of a "virtual synchronous machine", which is an inverter mimicking the response of a synchronous machine.

In order to provide a guide to the implementation of storage units into Kuramoto-like grids, which can serve as a starting point for follow-up research, we demonstrate basic control strategies adopted from electrical engineering and give insights into their potential and limitations with respect to different aspects of frequency quality improvement. The paper is organized as follows: First, we briefly address electrical storage in wind and solar applications and list the features of real storage units, which should be implementable into the model. Then, we outline Kuramoto-like power grid modeling and describe how to integrate storage units by means of load-flow equations. After that, we specify the simplified power system with realistic wind power input, which we use in this study. We close the subsection with an explanation of the frequency quality assessment we use and how this is related to established electrical engineering practice. Then, we turn to the application example: We start with a preliminary performance assessment by considering the ability to ensure stationary operation as a function of maximum capacity. Subsequently, we demonstrate how to implement three basic control strategies, namely, *state-of-charge feedback* reinterpreted as storage resource management, *droop control,* and *ramp-rate control.* We investigate their potential with respect to frequency quality improvement. It shows that these control concepts have different advantages according to their underlying main target. It is pointed out that the ambition in terms of control strength or tolerance range has to be carefully adjusted to the storage dimension in order to perform optimally. Finally, we demonstrate that these strategies are sensitive against finite-time response and confirm that short-term frequency quality applications require storage and control systems with rapid response. We conclude with a summary of the main results and give an outlook to storage-related problems, which can now be addressed within the context of Kuramoto-like power grid models.

## II. MODEL AND METHODS

### A. Electrical storage

Electrical energy storage[31] denotes the process of converting surplus electrical power into a storable form and reserving it, until it is converted back when required. It is commonly categorized by the form of energy stored but also in terms of its technical features like response time or capacity or its function. Electrical storage is already or considered as a promising candidate for various wind and solar power applications. The type of storage follows its function or, to be more precise, the underlying time scale of power variability. For long-term storage applications like time-shifting, peak-shaving, seasonal storage, and mid-term frequency control, storage types with large energy dimensions are used, which do not necessarily feature fast response, e.g., pumped hydro, hydrogen-based, or compressed air storage. Short-term frequency quality improvement and power output smoothing require rapid response (ranging from a few seconds to milliseconds), which is usually paralleled by smaller energy capacity. Candidates for this application are flywheels, batteries, superconducting magnetic energy storage, and (super) capacitors.[24,25]

The storage model to be developed has to meet two requirements: On the one hand, simplifications are essential in order to fit the model into the Kuramoto-like framework. On the other hand, all relevant characteristics of real storage operation have to be implementable, namely:[24,25,31]

- *Efficiency*
  In practice, the energy conversion processes cannot be realized without losses. The efficiency factor $\eta$ gives the ratio of input to output energy. It depends on the type of storage.
- *Maximum energy capacity* and *power rating*
  These define the main dimensions of the storage facility. The energy capacity is the maximum energy the storage unit is able to deliver and hence serves as an upper limit for the amount of energy stored. The power rating corresponds to the maximum instantaneous supply.
- *Control strategies*
  The storage-control strategy determines the storage output at time $t$ as a function of one or more feedback variables. It can be used to manage the storage resources or to provide system services like frequency control and power output smoothing.
- *Response time*
  The storage unit has a finite response time effecting a time delay between the feedback signal and its reaction. The response time depends on the type of storage and the underlying control mechanism.

### B. Kuramoto-like power grid models

Kuramoto-like grid models are based on networks of synchronous machines with producers (generators) and consumers (motors) converting mechanical power into electrical power and vice versa. Real and reactive power is transferred among these nodes via transmission lines. The topology of the underlying network is condensed in the nodal admittance matrix, $\{Y_{ij}\}_{i,j=1,\dots,N}$, with $N$ being the number of nodes. We adopt the common assumption of lossless transmission, i.e., neglectable conductances $G_{ij} = \mathfrak{Re}(Y_{ij})$, which yields $Y_{ij} \approx \mathrm{i}\mathfrak{Im}(Y_{ij}) = \mathrm{i}B_{ij}$ with susceptance $B_{ij}$. This assumption holds for transmission grids but not for the low and medium voltage level distribution grid or microgrids. (For a Kuramoto-like microgrid model including losses by means of phase shifts in the sinusoidal coupling term, see Auer *et al.*[21]) Each node $i \in \mathcal{M}_{\mathrm{grid}}$ of the grid is associated with a complex nodal voltage $\boldsymbol{E}_i = E_i \mathrm{e}^{\mathrm{i}\delta_i}$, with $E_i$ being the voltage magnitude and $\delta_i$ the phase with respect to a reference frame rotating with nominal frequency. (Hence, $\delta_i = \omega_i = 0$ means that node $i$ is at nominal frequency.)

The coupled frequency-voltage dynamics of the synchronous machines are given by[32,33]

$$m_i \ddot{\delta}_i = \gamma_i \dot{\delta}_i + P_i - \sum_{j=1}^{N} B_{ij} E_i E_j \sin \delta_{ij}, \tag{1a}$$

$$\alpha_i \dot{E}_i = C_i + \beta_i (\bar{E}_i - E_i) - E_i + \chi_i \sum_{j=1}^{N} B_{ij} E_j \cos \delta_{ij}. \tag{1b}$$

The parameters $m_i$ and $\gamma_i$ denote the total inertia and effective damping and $P_i$ is the mechanical power feed-in or consumption. $P_{ij} = B_{ij} E_i E_j \sin \delta_{ij}$ is the real power transfer between nodes $i$ and $j$, and the interaction term in Eq. (1b) is related to reactive power flows. $\alpha_i$, $C_i$, and $\chi$ can be calculated from machine parameters. The term $\beta_i(\bar{E}_i - E_i)$ mimics a proportional voltage controller, which pulls the voltage toward its nominal value.

In electrical engineering, the model given by Eqs. (1a) and (1b) is called a "one-axis model" or a "3rd order model", indicating that three differential equations $(\dot{\delta}, \dot{\omega}, \dot{E})$ are required. For a comprehensive discussion of the hierarchy of models ranging from 6th to 2nd order, see Machowski *et al.*[32] When introduced into the Kuramoto-like framework, Eqs. (1a) and (1b) were interpreted as a Kuramoto model with additional inertia plus a nontrivial time-dependent coupling term $K_{ij}(t) = B_{ij} E_i(t) E_j(t)$.[33]

While in Kuramoto-like modeling the consumer nodes are commonly treated as synchronous motors according to Eqs. (1a) and (1b), in electrical engineering the loads are often assumed to be constant admittances, which can be eliminated as passive nodes via Kron reduction.[32,34] Note that the model given by Eqs. (1a) and (1b) was derived for synchronous machines and does not hold for inverters, although it was shown that in the case of droop-controlled inverters, the dynamical equations can be formulated in a similar form.[35]

### C. Integration of storage units by means of load-flow equations

We now assume a power network consisting of a set of conventional synchronous machines $\mathcal{M}_{\mathrm{syn}}$ modeled according to Eqs. (1a) and (1b) and a set of storage units with control equipment $\mathcal{M}_{\mathrm{SCU}}$. The storage units are also associated with nodal voltages $\boldsymbol{E}_i = E_i \mathrm{e}^{\mathrm{i}\delta_i}$. However, their dynamics differ from synchronous machines in that they lack inertia and have no inherent physical relationship between frequency and electrical power output. The most direct approach, which does not include any restrictive assumptions on storage features or control, is to calculate the phase $\delta_i$, $i \in \mathcal{M}_{\mathrm{SCU}}$,

by solving the algebraic load-flow equation,[32,34]

$$P^{\text{out}}_{\text{SCU},i} = \sum_{j=1}^{N} B_{ij} E_i E_j \sin \delta_{ij}, \tag{2}$$

with the nodal voltage $E_i$ assumed to be constant. $P^{\text{out}}_{\text{SCU},i}$ is the power being injected into the grid by the storage-control unit.

Load-flow analysis is a standard tool in electrical engineering for power-flow calculations on power networks. It can be derived from basic physical relationships given by Kirchhoff's and Ohm's laws. This approach is particularly qualified as a starting point for the investigation of smart control since the power fed into the grid $P^{\text{out}}_{\text{SCU},i}$ can be determined by arbitrary control strategies and the model can flexibly be complemented with the other realistic storage characteristics listed above.

The algebraic equation (2) and the ordinary differential equations (1a) and (1b) form a system of differential-algebraic equations. The representation of a power system by differential-algebraic equations is standard in engineering, in particular, in so-called transient stability analysis.[32,36] This fact supports the combination of Kuramoto-like and load-flow equations as a method for the straightforward implementation of arbitrary grid components, e.g., power inverters and nodes linking different voltage levels or microgrid-macrogrid connections, into Kuramoto-like networks.

### D. Simplified power system with wind feed-in and storage facility

In this study, we demonstrate the operation of a storage unit with control equipment by means of a simplified system consisting of a generating unit with wind power feed-in and a synchronous machine mimicking the response of the grid in terms of frequency $\omega_{\text{sys}}$ and voltage $E_{\text{sys}}$ in a coarse-grained view (see Fig. 1). This inverter-motor system likewise represents a system composed of a wind power feed-in unit, a traditional generator, and ohmic loads, which have been eliminated by means of Kron reduction. We here consider its application with respect to frequency quality under fluctuating wind power feed-in.

The storage unit is assumed to have a finite maximum capacity $K_{\max}$. The actual capacity $K(t)$, or in more casual terms, the "filling level" at time $t$, corresponds to the *state of charge* with respect to batteries. $K_{\max}$ serves as an upper bound: if $K(t) = K_{\max}$, surplus energy cannot be stored and has to be discarded. On the other hand, the storage unit can only provide balancing power, if $K(t)$ is sufficient. For $K(t) = 0$, only positive power mismatch can be mitigated, whereas the system is exposed to negative power deficiencies.

For the sake of simplification, we neglect *efficiency* and limitations due to *power rating* here. This means that we assume lossless conversion and that the power to be delivered according to the specific control strategy is provided completely if permitted by the storage filling $K(t)$. The storage unit can be equipped with different control strategies. Three standard strategies adopted from engineering practice (*state-of-charge dependent resource management, droop control*, and *ramp-rate control*) are specified and investigated below. Our intention is to demonstrate the general impact of different basic storage strategies and their limitations due to maximum capacity and time-delay on system behavior rather than to model a detailed situation or derive concrete guidelines. The approach can be applied to more concrete situations in the course of follow-up research. Complex optimization problems may evolve depending on multiple factors such as operation conditions and technical system requirements, cost concerns, legal and economic framework, etc.

### E. Wind power feed-in

Due to atmospheric turbulence, wind power has specific turbulentlike characteristics:[4,37] extreme events, correlations, Kolmogorov power spectrum, and intermittent increment statistics. We implement realistic wind feed-in time series taking these basic properties into account,

$$P_{\text{WPP}}(t) = |P^{\text{cons}}_{\text{sys}}| + x(t), \tag{3}$$

with the constant part $|P^{\text{cons}}_{\text{sys}}|$ meeting the consumption of the system. The fluctuating time series $x(t)$ is generated as follows:[6] first, a time series $\tilde{x}(t)$ is generated by means of the Langevin-type system of equations,

$$\dot{y} = -\gamma y + \Gamma(t), \tag{4}$$

$$\dot{\tilde{x}} = \tilde{x}\left(g - \frac{\tilde{x}}{x_0}\right) + \sqrt{D\tilde{x}^2}\, y, \tag{5}$$

with $\gamma = 1.0$, $g = 0.5$, $x_0 = 2.0$, $D = 2.0$, and $\delta$-correlated Gaussian white noise $\Gamma$. Then, the corresponding Fourier spectrum is modified so that the final power spectrum $S(f) = |F(f)|^2$ roughly reproduces real data sets, in particular, the Kolmogorov $\frac{5}{3}$-decay. Transforming back to real space yields $x(t)$ [see Fig. 1(a) for an exemplary part of the feed-in time series $P_{\text{WPP}}(t)$]. Since $\langle x \rangle = 0$, power balance is given over time: $\langle P_{\text{WPP}} \rangle = |P^{\text{cons}}_{\text{sys}}|$. Due to the generating process, $P_{\text{WWP}}$ features a smallest frequency mode. Lower frequencies corresponding to power variations on longer time scales are assumed to be handled by other mechanisms like standard load balancing. In practice, different time scales can actually be divided up and assigned to different control mechanisms by low-pass filtering.[26]

### F. Power quality assessment

*Power quality* is a wide ranging notion, which includes different aspects of voltage, frequency stability, and supply reliability. In this study, we focus on short-term frequency quality. We use different criteria for performance assessment, which in combination give a more detailed picture of frequency quality.[38]

*Frequency quality*[5,7,39] refers to the systems ability to maintain nominal frequency $\omega^{\text{nom}}_{\text{sys}}$ or keep the frequency within a predefined range (the "standard frequency range") for a large percentage of operation time. It can be evaluated on different time scales. Short-term frequency quality is referred to "instantaneous frequency deviations" in electrical engineering. It is commonly evaluated by means of the percentage of time the system frequency is outside the standard frequency range.[39] Against this practical backdrop, we define

$$q_{\bar{\omega}} = \begin{cases} \int_{\bar{\omega}}^{\infty} p(\omega)\mathrm{d}\omega & \text{for } \bar{\omega} > 0, \\ \int_{-\infty}^{-\bar{\omega}} p(\omega)\mathrm{d}\omega & \text{for } \bar{\omega} < 0 \end{cases} \tag{6}$$

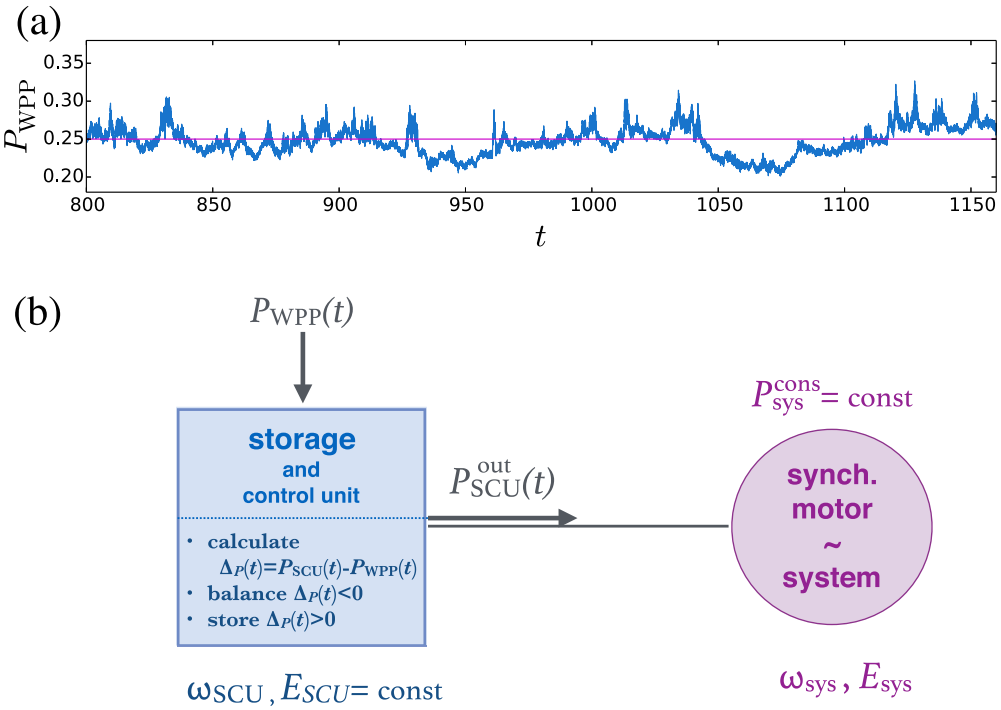


**FIG. 1.** Simplified model of a power system subjected to wind feed-in with local storage and control. (a) Exemplary part of the feed-in time series $P_{\mathrm{WPP}}(t) = |P^{\mathrm{cons}}_{\mathrm{sys}}| + x(t)$ delivered by a wind power plant or park [with $|P^{\mathrm{cons}}_{\mathrm{sys}}| = 0.25$ (magenta line), mean value $\langle x \rangle = 0$, and standard deviation $\sigma_x = 0.084 \cdot |P^{\mathrm{cons}}_{\mathrm{sys}}|$]. (b) On the basis of the actual wind power feed-in $P_{\mathrm{WPP}}(t)$, the Storage and Control Unit (SCU) first calculates the desired power output value $P_{\mathrm{SCU}}(t)$ according to the specific control strategy and the mismatch $\Delta_P(t) = P_{\mathrm{WPP}}(t) - P_{\mathrm{SCU}}(t)$. For $\Delta_P(t) < 0$, the mismatch is delivered by the storage, if the filling level $K(t)$ is sufficient. Conversely, surplus power $\Delta_P(t) > 0$ can only be stored with $K_{\mathrm{max}}$ as an upper bound. The power actually fed into the grid by the storage unit is denoted as $P^{\mathrm{out}}_{\mathrm{SCU}}(t) \leq P_{\mathrm{SCU}}(t)$. The "grid node" is modeled as a synchronous machine with parameters (following Ref. 6) read: $m = 1.0$, $\gamma = 0.2$, $P^{\mathrm{cons}}_{\mathrm{sys}} = -0.25$, $B_{12} = B_{21} = 1.0$, $B_{11} = B_{22} = -0.95$, $\alpha = 2.0$, $C = 0.9101$, $\beta = 1.0$, $\chi = 0.5$.

with $\bar{\omega}$ denoting the bound given by the standard frequency range $\omega^{\mathrm{nom}}_{\mathrm{sys}} \pm \bar{\omega}$ and $p(\omega)$ being the probability distribution of frequency deviations $\omega(t) = \omega_{\mathrm{sys}}(t) - \omega^{\mathrm{nom}}_{\mathrm{sys}}$. In real power grids, the nominal frequency is 50 Hz or 60 Hz. Kuramoto-like power grid models are usually transformed into a reference frame rotating with nominal frequency so that here, $\omega^{\mathrm{nom}}_{\mathrm{sys}} = 0$. For sufficiently long simulation, $q_{\bar{\omega}}$ corresponds to the percentage of time the system is expected to operate outside of the frequency range defined by $\bar{\omega}$ on average. For a specified standard frequency range $\pm\bar{\omega}$, $q_{|\bar{\omega}|} := q_{-\bar{\omega}} + q_{\bar{\omega}}$ corresponds to the "exceedance" measure introduced by Auer *et al.*[21] In this study, we evaluate $q_{\bar{\omega}}$ as a function of $\bar{\omega}$ rather than for one specified $\bar{\omega}$ for two reasons: firstly, this gives a more informative picture of system dynamics; secondly, the value of the standard frequency range is not unequivocally defined.[40]

Frequency quality not only involves deviations from nominal frequency, but also the time derivative $\mathrm{d}\omega/\mathrm{d}t$, commonly referred as the "rate of change of frequency."[7,39] The rate of change of frequency reflects the sensitivity against sudden perturbations and is inversely proportional to system inertia.[8] In former times, it was of interest mainly during transient periods after significant imbalances.[7] Nowadays, due to the loss of system inertia and the increasing percentage of stochastic renewables inducing continuous perturbations, the rate of frequency change becomes relevant also during *normal operation.*

The frequency changes can be related to the increments $\Delta\omega_{\mathrm{sys}} = \omega_{\mathrm{sys}}(t + \Delta t) - \omega_{\mathrm{sys}}(t)$. It was shown that intermittency of wind power in terms of heavy-tailed probability density functions is directly transferred into frequency fluctuations and significantly contribute to frequency quality decrease.[6] Therefore, we here capture increment statistics not only by their mean value $\mu_{|\Delta\omega|}$ and standard deviation $\sigma_{\Delta\omega}$ (as it is standard in electrical engineering) but also their kurtosis $\kappa_{\Delta\omega} = \mu_{4,\Delta\omega}/\sigma^4_{\Delta\omega}$ (with $\mu_4$ denoting the fourth moment of the distribution).[41] The kurtosis serves as a measure for the tailed-ness of the distribution. With $\kappa = 3$ being the value of the Gaussian distribution, $\kappa > 3$ means that there are more extreme events or outliers than in the Gaussian case and vice versa for $\kappa < 3$. Note that $\kappa$ entails information about the shape of the distribution, not about the magnitude of the outliers.

As we will see, the extreme events observed in the increment statistics in this study have two reasons: on the one hand, the system is exposed to the feed-in fluctuations $P_{\mathrm{WPP}}(t)$ during time intervals, in which the storage facility is not able or supposed to fully compensate power imbalances. As stated above, these fluctuations are known

to transfer intermittency into the frequency statistics. On the other hand, new extreme events can be induced when the storage steps in. For example, if the system runs out of storage in the course of a longer time period with power deficiency or discontinues balancing quite suddenly due to its control specifications, the frequency may face an instantaneous drop. The following analysis will show that the kurtosis serves as a good indicator for an inaccurate adjustment of control strength.

## III. RESULTS

### A. Storage control limited by maximum capacity

We assume the storage facility to have a maximum energy capacity $K_{\max}$. The actual power mismatch is $\Delta_P(t) = P_{\mathrm{WPP}}(t) - P_{\mathrm{SCU}}(t)$, with $P_{\mathrm{WPP}}(t)$ being the available wind power at time $t$ and $P_{\mathrm{SCU}}(t)$ the desired output power, which is supposed to be fed into the grid according to the underlying control scheme (see Fig. 1). However, the storage can balance power deficiencies only if the actual capacity $K(t)$ is sufficient, so that the power actually fed into the grid is $P^{\mathrm{out}}_{\mathrm{SCU}}(t) \leq P_{\mathrm{SCU}}(t)$.

In order to provide a first insight into the performance of the storage facility as a function of its maximum capacity, we first consider the simplified operation mode, in which the storage unit is intended to ensure power balance between feed-in and consumption whenever possible:

For positive power mismatch $\Delta_P(t) \geq 0$, $P^{\mathrm{out}}_{\mathrm{SCU}}(t) = |P^{\mathrm{cons}}_{\mathrm{sys}}|$ is fed into the system. The corresponding energy surplus $\Delta_K$ is stored with the maximum capacity $K_{\max}$ being an upper bound.
For $\Delta_P(t) < 0$, the power mismatch is

- either fully compensated, i.e., $P^{\mathrm{out}}_{\mathrm{SCU}}(t) = |P^{\mathrm{cons}}_{\mathrm{sys}}|$, if the storage is sufficiently filled,
- or the rest capacity is used to provide $P^{\mathrm{out}}_{\mathrm{SCU}}(t)$ with $P_{\mathrm{WPP}}(t) < P^{\mathrm{out}}_{\mathrm{SCU}}(t) < |P^{\mathrm{cons}}_{\mathrm{sys}}|$.
- While $K(t) = 0$, no balancing power can be provided.

In this mode of operation, the system dynamics alternate between stationary operation and time intervals with $\omega_{\mathrm{sys}} < 0$, in which the system either fluctuates in reaction to the stochastic feed-in or is on its way to return to stationary operation [see Fig. 2(a)]. Figure 2(b) shows how the percentage of nonstationary operation time $q_{\mathrm{nonstat}} = q_{|10^{-3}|}$[42] decreases to zero with maximum storage capacity $K_{\max}$.[43] The behavior for the $K \to \infty$ limit is trivial in qualitative respects, as it implies that a sufficiently large storage capacity is able to continually balance power differences and guarantee stationary operation. It was to be expected as we restricted our analysis to a limited time scale; i.e., we assumed the feed-in fluctuations to be balanced by other load control mechanisms on longer time scales.

However, our analysis so far was only to serve as a first storage capacity assessment. In reality, the equipment of wind and PV (photovoltaic) plants with large storage capacity is expensive. In the following, we, therefore, consider the more realistic and less trivial situation of a storage facility with "insufficient capacity."

### B. Storage-control strategies

We now investigate different basic storage-control strategies with regard to their potential to improve frequency quality. We set the maximum storage capacity $K_{\max} = 2.0$. This would allow for stationary operation in about 90% of time assuming the simplified strategy considered above. The control strategies refer to accepted methods in engineering practice and rely on different control feedback signals:

- the actual storage level $K(t)$ or the *state-of-charge* (here used for the purpose of "storage resource management"),
- system frequency as an indicator for power imbalances (*droop control*), and
- power differences between certain time steps (*ramp-rate control*).

These methods cover the elementary strategies for power quality improvement and, therefore, provide a basic structure for the development of smart control techniques by refining the conventional strategies or composing hybrid systems.

#### 1. Storage resource management

In the current technical application, the *state-of-charge* is applied as a feedback signal in battery storage systems mainly to guarantee operation within the proper state-of-charge range and to prevent shutdown due to overcharge.[27] Here, we shift the scope of application to the grid side and reinterpret the basic idea as a form of intelligent storage management.

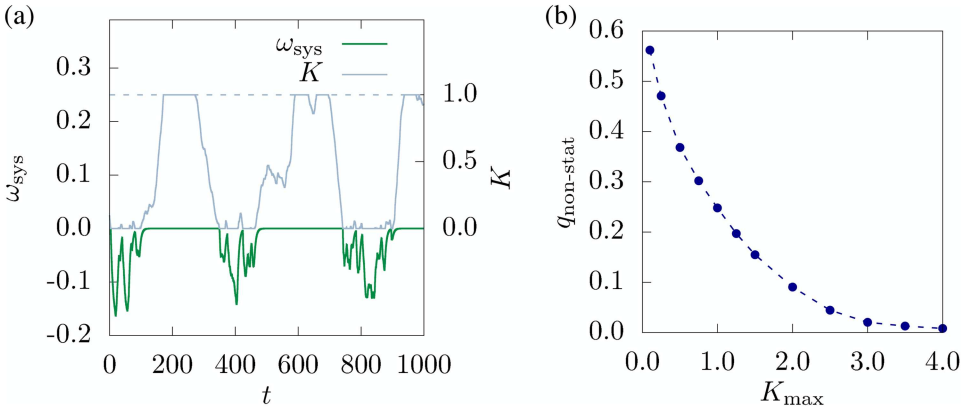


**FIG. 2.** Storage limited by maximum capacity $K_{\max}$. (a) Exemplary time series of system frequency $\omega_{\mathrm{sys}}(t)$ and storage filling level $K(t)$ for maximum storage capacity $K_{\max} = 1.0$. Empty or insufficient storage filling is paralleled by frequency fluctuations. (b) $q_{\mathrm{nonstat}} = q_{|10^{-3}|}$ gives the percentage of nonstationary operation.

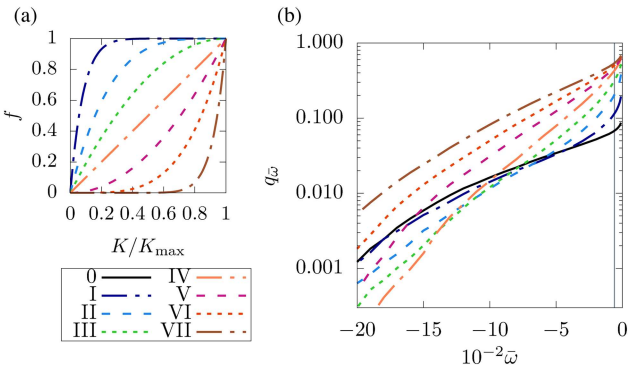


**FIG. 3.** Storage resource management for $K_{\max} = 2.0$. (a) Different realizations of storage resource management $f(K)$ denoted as strategies I–VII. "0" corresponds to the simplified storage mechanism with $f(K) = 1$. (b) $q_{\bar\omega}(\bar\omega)$ giving the percentage of time the system frequency is outside the $\bar\omega$ boundaries for realizations 0–VII. [As in the case described above, $\omega_{\text{sys}}(t) \leq 0$ in this mode of operation.]

We complement the simple storage strategy presented above and make the balance power at time $t$ dependent on the current capacity $K(t)$. To be specific, the power to be delivered by the storage is the power deficiency $\Delta_P$ multiplied by a factor $f = f(K(t)) \in [0, 1]$ with $f(0) = 0$ and $f(K_{\max}) = 1$. Here, we consider different realizations for $f(K)$ depicted in Fig. 3(a): $f(K) = -(1 - K/K_{\max})^n + 1$ for $n = 12, 4, 2$ (denoted as scenarios I, II, and III) and $f(K) = (K/K_{\max})^n$ for $n = 1, 2, 4, 12$ (scenarios IV–VII).

Figure 3(b) shows $q_{\bar\omega}(\bar\omega)$ for different realizations of storage resource management in comparison with the simplified storage strategy described in Subsection III A. With proper choice of $f(K)$, the proposed storage resource management can, in fact, serve to prevent large frequency deviations. Of course, a higher percentage of small deviations has to be tolerated in exchange. The best option can only be chosen in knowledge of the operational circumstances and the specific guidelines for $\bar\omega$. Furthermore, storage resource management can be applied as part of a multipronged control strategy in combination with other storage-control mechanisms.

### 2. Droop control

*Droop control* is based on the relationship between power imbalances and system frequency: a positive power mismatch is paralleled by frequency increase, whereas negative mismatch leads to frequency decrease. This fact can also be observed in Kuramoto-like grids.

Droop control has a broad range of application, which includes frequency control services provided by wind power plants.[26] The standard practice is to use a linear droop control mechanism, whose slope is given by the control strength $k_{\text{DC}}$. The balancing droop power is

$$P_{\text{droop}}(t) = k_{\text{DC}}(\omega_{\text{sys}}^{\text{nom}} - \omega_{\text{sys}}(t)) = -k_{\text{DC}}\omega(t), \tag{7}$$

as $\omega_{\text{sys}}^{\text{nom}} = 0$ here. If $\omega_{\text{sys}}(t) < 0$, this is interpreted as an indicator of negative power balance, and consequently, more power is injected into the system in order to keep system frequency close to its nominal value. For $\omega_{\text{sys}}(t) > 0$, power feed-in is reduced accordingly.

This adjustment of power input to the actual system frequency obviously requires storage capacity in the background. A specific type of inverter with linear droop control was shown to behave analog to a synchronous machine[44] and was already implemented into Kuramoto-like grids with stochastic feed-in.[21] Our approach here is different in the sense that we explicitly take into account the limits of the installed background storage capacity $K_{\max}$ but do not assume any further specifications on the grid feed-in process. As explained above, in the case of $\omega_{\text{sys}}(t) < 0$, the balancing power $P_{\text{droop}} > 0$ can only be provided to the extent that the storage level $K(t)$ is sufficient, and for $\omega_{\text{sys}}(t) > 0$, surplus power can only be stored with $K_{\max}$ as an upper bound.

We first investigate system performance under standard droop control according to Eq. (7) for fixed maximum storage capacity $K_{\max} = 2.0$ and varying control strength $k_{\text{DC}}$. Figure 4(a) shows system frequency in response to the same power feed-in $P_{\text{WPP}}(t)$ for different $k_{\text{DC}}$. With increasing control strength, the positive frequency deviations are more and more eliminated, as it is always possible to feed in less power than available. In contrast, balancing negative frequency deviations requires sufficient storage level. This asymmetry can also be seen in Fig. 4(b1), which reveals the dilemma of standard droop control under limited storage capacity: On the one hand, for sufficiently large control strength $k_{\text{DC}}$, the positive frequency deviations can be more or less eliminated, but in this case, the storage unit runs out of capacity quickly at the beginning of longer timer periods with negative power mismatch. Figure 4(a) highlights a concrete example of a frequency dip not being prevented due to overambitious control strength. On the other hand, for small control strength, the storage facility performs better in the sense that it reduces the probability of large negative frequency deviations. However, at the same time, the droop control mechanism remains suboptimal with respect to positive frequency deviations.

To overcome this problem, we propose a nonsymmetric droop control strategy, which treats positive and negative frequency deviations differently,

$$P_{\text{droop}}(t) = \begin{cases} -k_1^{\text{DC}}\omega_{\text{sys}}(t) & \forall\, \omega_{\text{sys}} \geq 0, \\ k_2^{\text{DC}}(\omega_{\text{sys}}(t))^n & \forall\, \omega_{\text{sys}} < 0. \end{cases} \tag{8}$$

We choose large control strength $k_1^{\text{DC}}$ in order to counteract the positive frequency deviations and tested two control schemes for the negative frequency range: (i) quartic droop control[45,55] and (ii) linear droop control with small control strength $k_2^{\text{DC}}$. Figure 4(b2) shows that these alternative strategies combine the best of both small and large control strength in standard droop control: they effectively mitigate positive deviations and prevent large frequency dips. A nonlinear control term, *inter alia*, gives the opportunity to focus the onset of control to a specific frequency bound. For example, the drop of $q_{\bar\omega}(\bar\omega)$ indicates that the quartic control term actually starts acting around $\omega_{\text{sys}} \approx 0.05$. For higher $n$, this would converge to a "dead band," i.e., a frequency range, in which the control system does not intervene.[46]

With a view to the frequency increment statistics [see Fig. 4(c)], the mean value $\mu_{|\Delta\omega|}$ and standard deviation $\sigma_{\Delta\omega}$ decrease with increasing control strength, finally converging to a minimum value.

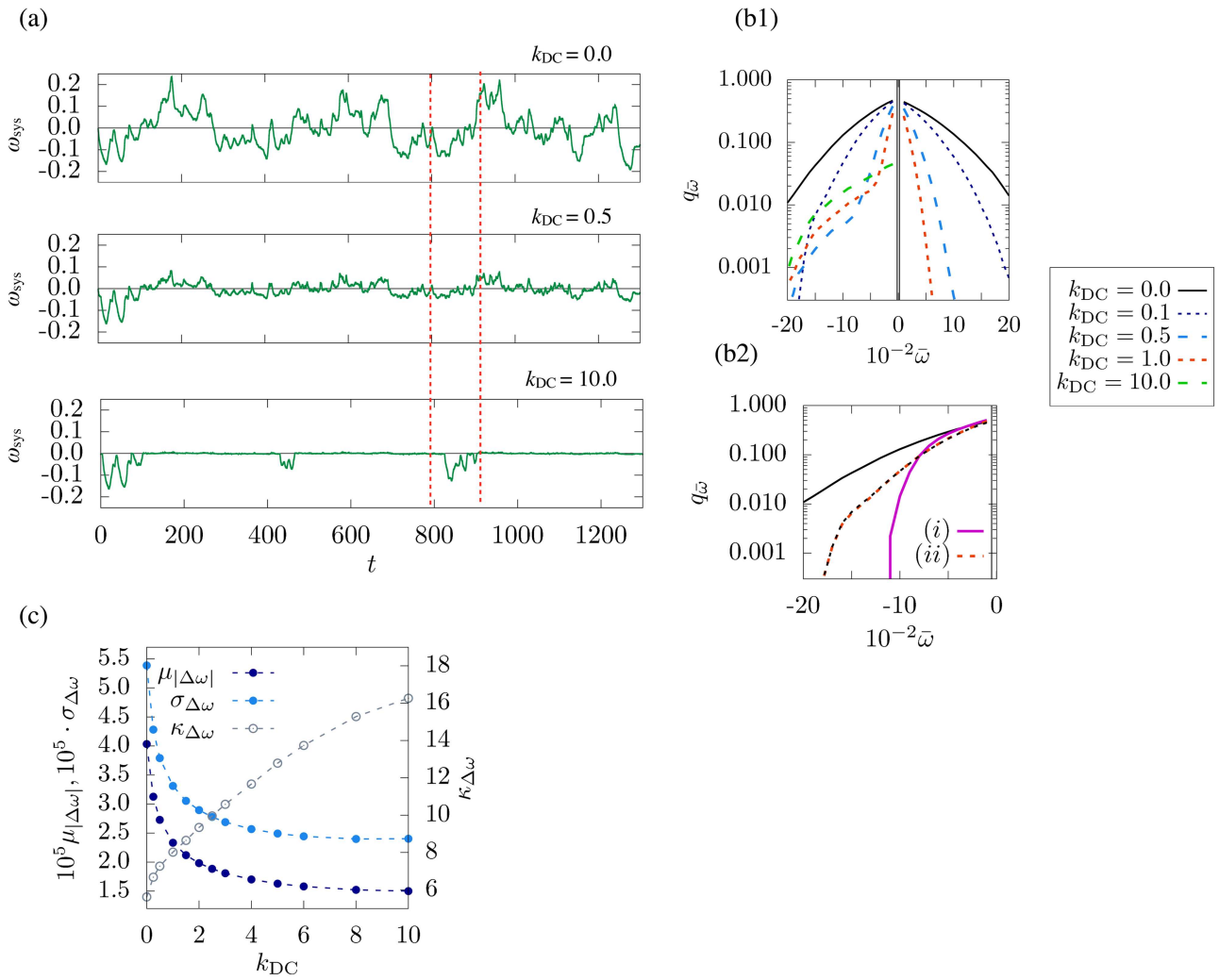


**FIG. 4.** Droop control with maximum storage capacity $K_{max} = 2.0$. (a) System frequency response to the same feed-in time series with standard droop control according to Eq. (7) for different control strengths $k_{DC} = 0.0$ (no control), $k_{DC} = 0.5$, and $k_{DC} = 10.0$. The time interval indicated by the red dotted lines illustrates the drawback of too ambitious control strength: the frequency dip is prevented for $k_{DC} = 0.5$ but no longer for $k_{DC} = 10.0$. (b1) $q_{\bar{\omega}}(\bar{\omega})$ for standard droop control with different control strengths $k_{DC}$. For $k_{DC} = 10.0$, the curve for positive deviations is not displayed due to its rapid decay [$q_{0.01}$ has already dropped to $\mathcal{O}(10^{-5})$]. (b2) $q_{\bar{\omega}}(\bar{\omega})$ for the alternative nonsymmetric droop control strategies according to Eq. (8): (i) $n = 4$, $k_2^{DC} = 10.0$, $k_2^{DC} = 200.0$ and (ii) $n = 1$, $k_2^{DC} = 10.0$, $k_2^{DC} = 0.1$. For negative $\bar{\omega}$, (ii) resembles the standard droop control case. (c) Increment statistics during nonstationary operation (according to the definition given above). For increasing $k_{DC}$ in standard droop control, the mean value $\mu_{|\Delta\omega|}$ and standard deviation $\sigma_\omega$ decrease, while the non-Gaussianity of the distribution in terms of the kurtosis $\kappa_{\Delta\omega}$ grows.

However, the non-Gaussianity in terms of kurtosis $\kappa_{\Delta\omega}$ grows, even when $\mu_{|\Delta\omega|}$ and $\sigma_{\Delta\omega}$ have nearly approached their minima and barely change.[47] This is an indicator that the control strength $k_{DC}$ is getting too ambitious and the storage facility runs out of capacity more frequently. It, therefore, becomes evident that increment statistics are an essential part of a comprehensive picture of frequency quality.

It should be noted that the control scheme we implemented here is a standard "grid-feeding" droop control strategy. There are other conceivable variants. For example, "grid-forming" inverters introduce a novel control algorithm, which is currently discussed against the background of progressive renewable energy integration.[48,49]

### 3. Ramp-rate control

A *power ramp* is defined as a normalized power change or power increment,

$$\Delta P_{ramp}(t) = \frac{P_{in}(t) - P_{ref}}{P_{norm}}, \tag{9}$$

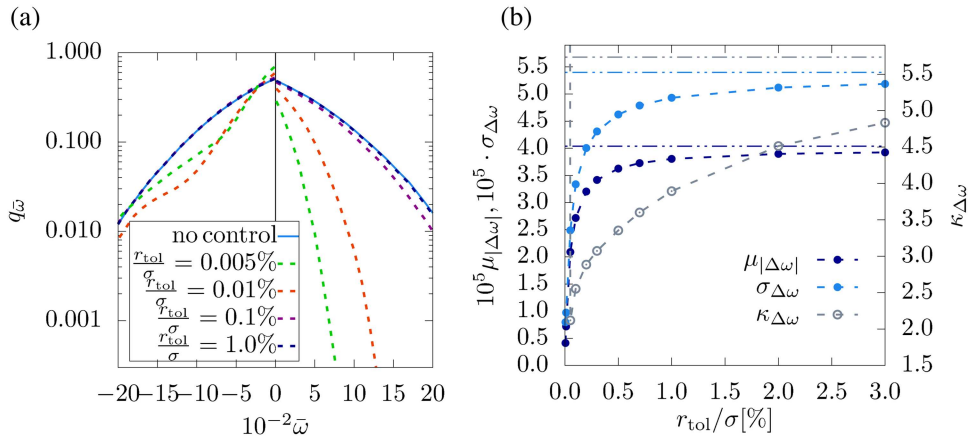


**FIG. 5.** Ramp-rate control with $K_{max} = 2.0$. (a) $q_{\bar{\omega}}(\bar{\omega})$ for different tolerance ramp rates $r_{tol}$ given in percent of the standard deviation of the wind power feed-in $\sigma$. (b) Increment statistics during nonstationary operation: with decreasing ramp tolerance $r_{tol}$, frequency increments are mitigated in terms of their mean value $\mu_{\Delta\omega}$, standard deviation, and kurtosis $\kappa_{\Delta\omega}$. For large tolerance ramps, the influence of control diminishes and $\mu_{\Delta\omega}$, $\sigma_{\Delta\omega}$, and $\kappa_{\Delta\omega}$ approach their values of the no-control case (horizontal lines).

with input power $P_{in}(t)$ and reference power $P_{ref}$. *Ramp-rate control*[50,51] aims at keeping power ramps within specified tolerance bounds,

$$|\Delta P_{ramp}| \leq r_{tol}. \tag{10}$$

It is utilized in wind and solar power applications. In the latter case, power ramps play a even major role due to passing clouds.

The basic idea opens up numerous opportunities for concrete realization depending on the choice of $P_{ref}$. For example, it can be given by prior values $P(t - \Delta t)$ defined by a sampling time $\Delta t$ or be calculated as a function of the actual demand. We here demonstrate a version of ramp-rate control, which mainly targets on short-term ramps: First, we set $P_{ref} = P^{out}_{SCU}(t - \Delta t)$ with $\Delta t = 0.005$. As long as the ramp condition [Eq. (10)] is satisfied, no balancing is necessary, and $P^{out}_{SCU}(t) = P_{WPP}(t)$. If the condition is violated, the storage facility steps in: For $\Delta P_{ramp} > 0$ (upward ramps), $P^{out}_{SCU}$ is decreased so that $|\Delta P_{ramp}| = r_{tol}$ and surplus power is stored. For $\Delta P_{ramp} < 0$ (downward ramps), the storage is supposed to provide balance power in order to fulfill $|\Delta P_{ramp}| = r_{tol}$. Again, the storage of surplus power is limited by the maximum capacity $K_{max}$, and balancing power can only be delivered if the actual storage level $K(t)$ is sufficient.

The performance of ramp-rate control is usually assessed with respect to the power feed-in statistics. Here, we consider frequency statistics instead, for two reasons: first, this is the scope of our study and consistent with the previous analysis. Second, we investigate a consequential phenomenon, as power fluctuations are directly transferred into frequency variations. Figures 5(a) and 5(b) show how the likelihood of tolerance bound violations in terms of $q_{\bar{\omega}}(\bar{\omega})$ and the frequency increment statistics evolve as functions of the tolerance ramp rate $r_{tol}$. It shows that the ramp-rate control strategy fulfills its main purpose with a view to the increment statistics: by suppressing power ramps, frequency increments can be mitigated significantly. In parallel, the percentage of operation time beyond certain tolerance bounds can be decreased.

Again, the ambition of control, here in terms of $r_{tol}$, has to be chosen carefully. On the one hand, if $r_{tol}$ is too large, the control does not achieve its potential. It has no influence on $q_{\bar{\omega}}(\bar{\omega})$ and barely improves the increment statistics. On the other hand, if $r_{tol}$ is too small, the storage tends to run out of capacity. This is indicated by a steep rise of $\kappa_{\Delta\omega}$ and increasing likelihood of large negative frequency deviations. Compounding the problem in this specific version of *ramp-rate control* is the fact that if the power input $P^{out}_{SCU}$ drops to a low $P_{WPP}$ during a feed-in deficit period with empty storage, this value serves as the new reference $P_{ref}$. In the following, the input power and system frequency can return to their nominal values only slowly due to the tight tolerance range, even if storage capacity is available. As explained before, running out of storage is paralleled by sudden frequency drops, which is indicated by the drastic increase of the non-Gaussianity of the increment distribution.

Note that the dissymmetry between positive and negative frequency deviations [which can be seen in Fig. 5(a)] is not completely analog to the droop control case. First, ramp-rate control responds to power input fluctuations (which cause frequency fluctuations) and not to the deviation from nominal frequency directly. Second, upward ramps can always be balanced, irrespective of whether the actual system frequency is below or above its nominal value. In contrast, balancing downward ramps requires sufficient storage. This particularly affects power deficit periods accompanied by $\omega_{sys} < 0$, during which the storage is depleted.

Comparing droop control and the applied version of ramp-rate control, the latter has the advantage to be able to mitigate frequency increments to a certain extent without being paralleled by increasing non-Gaussianity. For example, droop control with $k_{DC} = 6.0$ and ramp control with $r_{tol} = 0.03\sigma\%$ both reduce the mean value to $\mu_{\Delta\omega} \approx 1.6 \cdot 10^{-5}$. At the same time, the statistics for the droop control case contain considerably more extreme events ($\kappa_{\Delta\omega} = 13.7$)

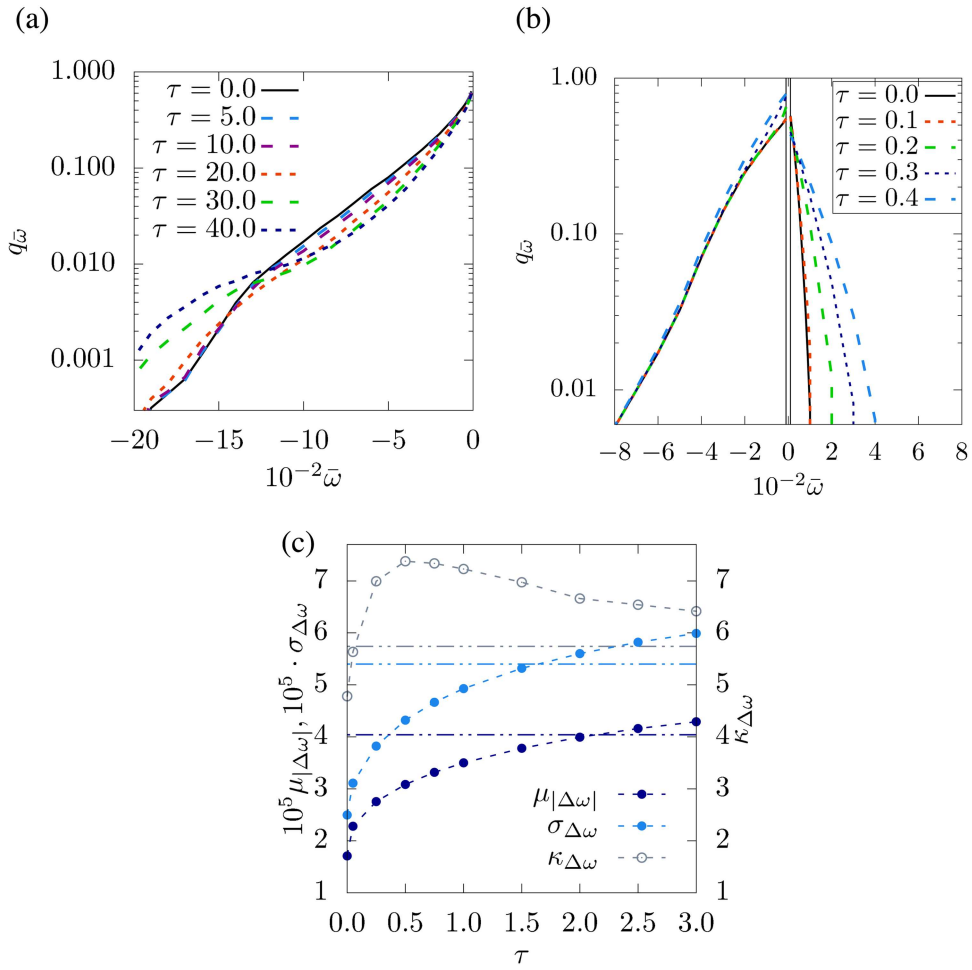


**FIG. 6.** How finite response time undermines frequency quality improvement. (a) Linear storage resource management: $q_{\bar{\omega}}(\bar{\omega})$ for different response times $\tau$. The curves for $\tau < 5.0$ almost resemble the instantaneous-response ($\tau = 0$) case. (b) Droop control for the asymmetric control strategy (ii). Again, $q_{\bar{\omega}}(\bar{\omega})$ is shown for different response times. For $\tau < 0.1$, the impact of finite-time response on $q_{\bar{\omega}}(\bar{\omega})$ is negligible. (c) Increment statistics for ramp-rate control as a function of $\tau$. The horizontal lines indicate the values for the no-control case.

than the system with the ramp rate mechanism ($\kappa_{\Delta\omega} = 1.8$). On the other hand, the ramp-rate control does not take into account the absolute deviation from nominal frequency and hence is not designed to prevent large frequency excursion as efficiently as droop control.

### C. Finite response time

Each electrical storage technology is associated with a characteristic response time ranging from minutes (e.g., pumped hydro, compressed air, liquid air) to milliseconds, e.g., batteries, (super) capacitors, superconducting magnetic energy storage.[26] In combination with their characteristic capacity, they are suitable for different storage applications (see Sec. II A). In the following, we investigate and compare the sensitivity of the three control strategies introduced in Sec. III B. We implemented finite-time response assuming that the control does not react instantaneously but in response to the feedback signal at time $t - \tau$. (Alternatively, the time delay could be modeled by ordinary differential equations with appropriate time constants; e.g., see Schiffer *et al.*[35]):

- In the case of *storage resource management*, the balance power to be delivered by the storage facility is $\Delta_P \cdot f(K(t-\tau))$.[52] We picked the linear storage resource management scenario VI as an example.
- For *droop control*, we instance the asymmetric control strategy (ii) with $k_1^{\mathrm{DC}} = 10.0$ and $k_2^{\mathrm{DC}} = 0.5$. The balancing power $P_{\mathrm{droop}}(t)$ is calculated on the basis of $\omega_{\mathrm{sys}}(t-\tau)$.
- The *ramp-rate control* realization we presented above is very sensitive due to the short sampling rate. In view of finite-time

response, we consider another variant of ramp rate control and define the reference power $P_{\mathrm{ref}} = |P_{\mathrm{sys}}^{\mathrm{cons}}|\ \forall t$ and the tolerance range $r_{\mathrm{tol}} = 0.5\sigma$ here. The balancing power at time $t$ is calculated as the response to $\Delta P_{\mathrm{ramp}}(t-\tau)$.

Figure 6 shows how time delay limits the possibilities for frequency quality improvement with focus on the main target of each control strategy.

Storage resource management was introduced in order to prevent overspending and save capacity to mitigate large frequency deviations. From Fig. 6(a), one can see that finite response time has negligible impact up to $\tau = 10.0$. Then, the deviations from the instantaneous-response case become more and more apparent. In particular, the control strategy increasingly misses its main objective as the probability of large deviations from nominal frequency grows.

Droop control is intended to mitigate deviations from nominal frequency. Figure 6(b) shows that in this respect, the system is able to handle a finite response time up to $\tau = 0.1$ quite well. Then, $q_{\bar{\omega}}$ starts to increase for small $\bar{\omega}$ as the feedback delay causes trouble when the system fluctuates close around nominal frequency. As the control switches between positive and negative balancing too late, oscillations around nominal frequency are induced. A nonlinear droop scheme could mitigate these oscillations as it interferes less for small deviations.

Ramp-rate control was shown to be a promising candidate for frequency quality improvement with respect to increment statistics. The version of ramp-rate control considered here is very sensitive toward time delay. Figure 6(c) shows that the introduction of finite response time leads to a reduction of frequency quality as $\mu_{|\Delta\omega|}$, $\sigma_{\Delta\omega}$, and $\kappa_{\Delta\omega}$ immediately increase, even beyond the no-control case.

These results indicate that short-term frequency quality applications require rapid response times (on the subsecond scale[53]). It shows that control strategies targeting the fast fluctuations are sensitive even against "near to instantaneous response", as the smallest delays in the order of milliseconds are classified.[26] As these systems are usually expensive, it may be advisable to use hybrid systems and treat the high-frequency and lower frequency fluctuations separately with different storage and control systems.

## IV. DISCUSSION AND OUTLOOK

We extended the current Kuramoto-like modeling framework with flexible storage units. With that, the scope of Kuramoto-like models opens up to one of the most important research topics in power grid engineering. On the way to this goal, we brought together Kuramoto-like equations and load-flow analysis. This is a substantial extension, supported by standard engineering practice, which can serve as a starting point for the straightforward implementation of arbitrary grid components into Kuramoto-like grids.

For demonstration purposes, we considered short-term frequency quality improvement by means of storage facility with maximum capacity in a power system subjected to realistic wind feed-in. Motivated by recent findings, we assessed system performance not only with respect to frequency range violations, but also took into account frequency increment statistics.

We demonstrated how to implement three basic control methods, which cover the elementary strategies for power quality improvement in engineering practice. First, we adopted *state-of-charge feedback control* and reinterpreted it as a form of storage resource management. It has been proven that this concept can actually serve to save capacity in order to prevent large frequency deviations. Second, it was shown that *droop control* can improve frequency quality not only with a view to deviations from nominal frequency but also with respect to frequency increment statistics. We pointed out that, particularly in the case of limited capacity, it is favorable to handle positive and negative frequency deviations with different droop schemes and consider nonlinear mechanisms. Third, we implemented a version of "ramp-rate control." Originally designed for power-output-smoothing applications, we demonstrated that this strategy entails frequency quality improvement.

For both droop and ramp-rate control, it became apparent that the corresponding control strength or ramp tolerance range may not be too ambitious and have to be carefully proportioned to the dimensions of the storage facility. Furthermore, it was shown that the finite response time of the control mechanism limits the potential of the storage facility. Short-term frequency quality applications, in particular, require a rapid response.

With this study, we created a sound starting point for follow-up research on various aspects of storage implementation from the viewpoint of self-organized synchronization and collective phenomena. This includes stability-topology issues like *optimal siting* of storage units as well as comparative studies on global vs local storage location or *optimal sizing* and rough cost-benefit assessment. Another current topic is the development and refinement of smart control strategies, which are customized to the realistic features of wind and solar power and, at the same time, take into account the impact of collective network dynamics. This study has already shown that the presented basic control strategies have different advantages and disadvantages. Against this backdrop, and with a view to the impact of finite response times, systems with combined control techniques are conceivable solutions, and novel smart control strategies should be developed.

## ACKNOWLEDGMENTS

Financial support from the Deutsche Forschungsgemeinschaft (DFG) (Grant Nos. PE 478/16-1 and MA 1636/9-1) is gratefully acknowledged.

## REFERENCES

[1] M. H. Albadi and E. F. El-Saadany, "Overview of wind power intermittency impacts on power systems," Electric Power Syst. Res. **80**, 627–632 (2010).
[2] H. Ibrahim, M. Ghandour, M. Dimitrova, A. Ilinca, and J. Perron, "Integration of wind energy into electricity systems: Technical challenges and actual solutions," Energy Procedia **6**, 815–824 (2011).
[3] G. Ren, J. Liu, J. Wan, Y. Guo, and D. Yu, "Overview of wind power intermittency: Impacts, measurements, and mitigation solutions," Appl. Energy **204**, 47–65 (2017).
[4] M. Anvari, G. Lohmann, M. Wächter, E. Lorenz, D. Heinemann, W. R. R. Tabar, and J. Peinke, "Short term fluctuations of wind and solar power systems," New J. Phys. **18**, 063027 (2016).
[5] "Policy 1: Load-frequency control and performance [C]," in *Continental Europe Operation Handbook* (ENTSO-E (UCTE), 2009).
[6] K. Schmietendorf, J. Peinke, and O. Kamps, "The impact of turbulent renewable energy production on power grid stability and quality," Eur. Phys. J. B **90**, 222 (2017).

[7]"High Penetration of Power Electronic Interfaced Power Sources (HPo3PEIPS)—ENTSO-E guidance document for national implementation for network codes on grid connection" (ENTSO-E, 2017).
[8]P. Tielens and D. Van Hertem, "Grid inertia and frequency control in power systems with high penetration of renewables," in *Young Researchers Symposium in Electrical Power Engineering* (IEEE, 2012).
[9]F. Milano, F. Döfler, G. Hug, D. J. Hill, and G. Verbič, "Foundations and challenges of low-inertia systems," in *2018 Power Systems Computation Conference (PSCC)* (IEEE, 2018), pp. 1–25.
[10]Y. Kuramoto, "Self-entrainment of a population of coupled non-linear oscillators," in *International Symposium on Mathematical Problems in Theoretical Physics* (Springer, 1975), Vol. 39, pp. 420–422.
[11]S. H. Strogatz, "From Kuramoto to Crawford: Exploring the onset of synchronization in populations of coupled oscillators," Physica D **143**, 1–202 (2000).
[12]G. Filatrella, A. H. Nielsen, and N. F. Pedersen, "Analysis of a power grid using a Kuramoto-like model," Eur. Phys. J. B **61**, 485–491 (2008).
[13]P. J. Menck, J. Heitzig, J. Kurths, and H. J. Schellnhuber, "How dead ends undermine power grid stability," Nat. Commun. **5**, 3969 (2014).
[14]A. E. Motter, S. A. Myers, M. Anghel, and T. Nishikawa, "Spontaneous synchrony in power-grid networks," Nat. Phys. **9**, 191–197 (2013).
[15]M. Rohden, A. Sorge, M. Timme, and D. Witthaut, "Self-organized synchronization in decentralized power grids," Phys. Rev. Lett. **109**, 064101 (2012).
[16]M. Rohden, D. Jung, S. Tamrakar, and S. Kettemann, "Cascading failures in ac electricity grids," Phys. Rev. E **94**, 032209 (2016).
[17]M. Rohden, D. Witthaut, M. Timme, and H. Meyer-Ortmanns, "Curing critical links in oscillator networks as power flow models," New J. Phys. **19**, 013002 (2017).
[18]D. Witthaut, M. Rohden, X. Zhang, S. Hallerberg, and M. Timme, "Critical links and nonlocal rerouting in complex supply networks," Phys. Rev. Lett. **116**, 138701 (2016).
[19]M. Wolff, P. G. Lind, and P. Maass, "Power grid stability under perturbation of single nodes: Effects of heterogeneity and internal nodes," Chaos **28**, 103120 (2018).
[20]H. Haehne, J. Schottler, M. Waechter, J. Peinke, and O. Kamps, "The footprint of atmospheric turbulence in power grid frequency measurements," Europhys. Lett. **121**, 30001 (2018).
[21]S. Auer, F. Hellmann, M. Krause, and J. Kurths, "Stability of synchrony against local intermittent fluctuations in tree-like power grids," Chaos **27**, 127003 (2017).
[22]X. Zhang, "Dynamic responses of networks under perturbations: Solutions, patterns and predictions," Ph.D. thesis (Georg-August-Universität Göttingen, 2017).
[23]B. Schäfer, M. Matthiae, X. Zhang, M. Rohden, M. Timme, and D. Witthaut, "Escape routes, weak links, and desynchronization in fluctuation-driven networks," Phys. Rev. E **95**, 060203 (2017).
[24]F. Díaz-González, A. Sumper, O. Gomis-Bellmunt, and R. Villafáfila-Robles, "A review of energy storage technologies for wind power applications," Renewable Sustainable Energy Rev. **16**, 2154–2171 (2012).
[25]M. Jabir, H. Azil Illias, S. Raza, and H. Mokhlis, "Intermittent smoothing approaches for wind power output: A review," Energies **10**, 1572 (2017).
[26]H. Zhao, Q. Wu, S. Hu, H. Xu, and C. N. Rasmussen, "Review of energy storage system for wind power integration support," Appl. Energy **137**, 545–553 (2015).
[27]X. Li, D. Hui, and X. Lai, "Battery energy storage station (BESS)-based smoothing control of photovoltaic (PV) and wind power generation fluctuations," IEEE Trans. Sustain. Energy **4**, 464–473 (2013).
[28]D. Lee, J. Kim, and R. Baldick, "Stochastic optimal control of the storage system to limit ramp rates of wind power output," IEEE Trans. Smart Grid **4**, 2256–2265 (2013).
[29]N. Hamsic, A. Schmelter, A. Mohd, E. Ortjohann, E. Schultze, A. Tuckey, and J. Zimmermann, "Increasing renewable energy penetration in isolated grids using a flywheel energy storage system," in *2007 International Conference on Power Engineering, Energy and Electrical Drives* (2007), pp. 195–200.
[30]R. Hesse, D. Turschner, and H.-P. Beck, "Micro grid stabilization using the virtual synchronous machine (VISMA)," Renewable Energy Power Quality J. **1**, 676–681 (2009).
[31]X. Luo, J. Wang, M. Dooner, and J. Clarke, "Overview of current development in electrical energy storage technologies and the application potential in power system operation," Appl. Energy **137**, 511–536 (2015).
[32]J. Machowski, J. Bialek, and D. Bumby, *Power System Dynamics: Stability and Control* (John Wiley & Sons, 2008).
[33]K. Schmietendorf, J. Peinke, O. Kamps, and R. Friedrich, "Self-organized synchronization and voltage stability in networks of synchronous machines," Eur. Phys. J. Special Topics **223**, 2577–2592 (2014).
[34]P. Kundur, N. J. Balu, and M. G. Lauby, *Power System Stability and Control* (McGraw-Hill, 1994).
[35]J. Schiffer, R. Ortega, A. Astolfi, J. Raisch, and T. Sezi, "Conditions for stability of droop-controlled inverter-based microgrids," Automatica **50**, 2457–2469 (2014).
[36]X.-F. Wang, Y. Song, and M. Irving, *Modern Power System Analysis* (Springer US, 2008).
[37]P. Milan, M. Wächter, and J. Peinke, "Turbulent character of wind energy," Phys. Rev. Lett. **110**, 138701 (2013).
[38]Electrical engineering literature indicates "power output smoothing" as another major issue with respect to stochastic feed-in.[25,27] This is related to frequency quality, as system frequency and power balance are coupled.
[39]"Supporting Document for the Network Code on Load-Frequency Control and Reserves" (ENTSO-E, 2013).
[40]In the ENTSO-E report for the network code on load-frequency control and reserves,[40] this fact is mentioned with a view to the different characteristics of transmission grid areas. This applies even more for the heterogeneous operation conditions on the distribution grid level and in islanded microgrids.
[41]The statistical measures $\mu_{|\Delta\omega|}$, $\sigma_{\Delta\omega}$, and $\kappa_{\Delta\omega}$ refer to a given time lag $\Delta t$; i.e., strictly speaking, we have $\mu^{\Delta t}_{|\Delta\omega|}$, etc. We drop the upper index but specify $\Delta t$ in the following analysis.
[42]We define $|\omega_{\mathrm{sys}}(t)| < |10^{-3}|$ as stationary operation. This is in accordance with real power grids in the sense that, strictly speaking, these are constantly subjected to disturbances and hence never in a stationary state with $\omega_{\mathrm{sys}} = \omega^{\mathrm{nom}}_{\mathrm{sys}}$ and $\frac{\mathrm{d}}{\mathrm{d}t}\omega_{\mathrm{sys}} = 0$.
[43]We set $K(0) = 0.1 \cdot K_{\mathrm{max}}$ here and $K(0) = 0.1$ in the following simulations performed with fixed $K_{\mathrm{max}} = 2.0$. We additionally gave the system a settling time, before we started to collect data, in order to make the statistics comparable.
[44]J. Schiffer, D. Goldin, J. Raisch, and T. Sezi, "Synchronization of droop-controlled microgrids with distributed rotational and electronic generation," in *52nd IEEE Conference on Decision and Control* (IEEE, 2013).
[45]Nonlinear droop control is technically feasible.[55]
[46]T. Ono and J. Arai, "Frequency control with dead band characteristic of battery energy storage system for power system including large amount of wind power generation," Electric. Eng. Jpn. **185**, 1–10 (2013).
[47]The corresponding values of the statistical measures for the alternative strategies (i) and (ii) are as follows: (i) $\mu_{|\Delta\omega|} = 2.25 \cdot 10^{-5}$, $\sigma_{\Delta\omega} = 3.21 \cdot 10^{-5}$, $\kappa_{\Delta\omega} = 9.00$ and (ii) $\mu_{|\Delta\omega|} = 2.26 \cdot 10^{-5}$, $\sigma_{\Delta\omega} = 3.16 \cdot 10^{-5}$, $\kappa_{\Delta\omega} = 8.50$.
[48]P. Unruh, R. Brandl, M. Jung, and A. Seibel, "Enhanced grid-forming inverters in future power grids," in *20th European Conference on Power Electronics and Applications (EPE'18 ECCE Europe), Riga, Latvia, 17–21 September 2018* (IEEE, 2018).
[49]I. Serban and C. P. Ion, "Microgrid control based on a grid-forming inverter operating as virtual synchronous generator with enhanced dynamic response capability," Int. J. Electric. Power Energy Syst. **89**, 94–105 (2017).
[50]J. Marcos, O. Storkël, L. Marroyo, M. Garcia, and E. Lorenzo, "Storage requirements for PV power ramp-rate control," Solar Energy **99**, 28–35 (2014).
[51]J. Schnabel and S. Valkealahti, "Energy storage requirements for PV power ramp rate control in Northern Europe," Int. J. Photoenergy **2016**, 2863479.
[52]We here assumed finite-time response solely for the filling-level feedback, while the calculation of $\Delta_P$, and hence the decision whether the storage facility has to step in, happens instantaneously in response to the actual mismatch $\Delta_P(t)$. If this was not the case (this process would perhaps be associated with another time delay $\tau'$), the situation would of course be exacerbated and also positive frequency deviations could occur.
[53]As we use a greatly simplified power system in dimensionless units in order to point out general relationships, we are careful with specifying concrete values.

However, at this point, we want to give a rough idea about the time scale. For $\mathcal{O}(m) \sim 10^4\,\mathrm{kg\,m^2}$, $\omega_{\mathrm{sys}}^{\mathrm{nom}} = 2\pi \cdot 50\,\mathrm{Hz}$, $\mathcal{O}(BE_{\mathrm{sys}}E_{\mathrm{SCU}}) \sim 1\,\mathrm{GW}$, and $\mathcal{O}(1/\gamma) \sim 0.1\,\mathrm{s}$–$1\,\mathrm{s}$ (cf. Ref. 13), $t = \mathcal{O}(t) \sim 0.1\,\mathrm{s}$–$1\,\mathrm{s}$, and hence, the response time of the storage facility has to be in the subsecond range. This coarse evaluation is in accordance with the technical features of electrical storage with the fastest response times being in the range of milliseconds.[26]

[54]B. Schäfer, C. Beck, K. Aihara, D. Witthaut, and M. Timme, "Non-Gaussian power grid frequency fluctuations characterized by Lévy-stable laws and superstatistics," Nat. Energy **3**, 119–126 (2018).
[55]P. Prabhakaran, Y. Goyal, and V. Agarwal, "Novel nonlinear droop control techniques to overcome the load sharing and voltage regulation issues in DC microgrid," IEEE Trans. Power Electron. **33**, 4477–4487 (2018).